

Point-contact spectroscopy in MgB₂ single crystals in magnetic field

D. Daghero^{a*}, R.S. Gonnelli^a, G.A. Ummarino^a, V.A. Stepanov^b, J. Jun^c, S.M. Kazakov^c, and J. Karpinski^c

^aINFM - Dipartimento di Fisica, Politecnico di Torino, Corso Duca degli Abruzzi 24, 10129 Torino, Italy

^bP.N. Lebedev Physical Institute, Russian Academy of Sciences, Leninski Pr. 53, 119991 Moscow, Russia

^cSolid State Physics Laboratory, ETH, CH-8093 Zürich, Switzerland

We present the results of a spectroscopic study of state-of-the-art MgB₂ single crystals, carried out by using a modified point-contact technique. The use of single crystals allowed us to obtain point contacts with current injection either parallel or perpendicular to the *ab* planes. The effect of magnetic fields up to 9 T on the conductance spectra of these contacts is here thoroughly studied, for both **B** parallel and perpendicular to the *ab* planes. The complete thermal evolution of the upper critical field of the π band is determined for the first time, and quantitative information about the upper critical field of the σ band and its anisotropy is obtained. Finally, by exploiting the different effect of a magnetic field applied parallel to the *ab* planes on the two band systems, the partial contributions of the σ and π bands to the total conductance are obtained separately. Fitting each of them with the standard BTK model yields a great reduction of the uncertainty on Δ_σ and Δ_π , whose complete temperature dependence is obtained with the greatest accuracy.

1. Introduction

About two years after the discovery of superconductivity in MgB₂, the validity of the two-gap model [1,2,3,4] in describing the superconducting and normal-state properties of this material has been confirmed by a large number of experimental evidences. Within this model, the complex electronic bandstructure of MgB₂ [5,6,7,8] is approximated by one quasi-2D σ band and one 3D π band, featuring two gaps of very different amplitude, Δ_σ and Δ_π . The different spatial character of the two bands arises from the layered structure of the material, that is also expected to give rise to macroscopic anisotropy in some relevant physical quantities, e.g. penetration depth, coherence length, and upper critical fields. The value of the anisotropy ratio $\gamma = H_{c2}^{ab}/H_{c2}^c$ in MgB₂ has long been a matter of debate, because of the large spread of values measured in films and polycrystalline samples [9]. To this regard, the recent set-up of efficient crystal-growth techniques has thus been an essential improvement. As a matter of

fact, torque magnetometry [10] and thermal conductivity measurements [11] in high-quality single crystals have given substantially consistent values of the upper critical fields as a function of the temperature.

In this paper, we present the results of directional point-contact spectroscopy (PCS) in state-of-the-art single crystals, in the presence of a magnetic field applied either parallel or perpendicular to the *ab* planes. The use of PCS, and the possibility of controlling the directions of both the injected current and the field, allowed us to study the effect of the magnetic field on each band system, separately. It turns out that the magnetic field strongly affects the superconductivity in the π -band, irrespective of its orientation. An analysis of the conductance curves measured at different temperatures and various field intensities gives the temperature evolution of the π -band upper critical field, $B_{c2}^\pi = \mu_0 H_{c2}^\pi$, determined here for the first time. In contrast, the effect of the field on the σ band is highly anisotropic. Our measurements indicate that the upper critical field of the σ band for **B** parallel to the *c*

*Corresponding author. e-mail: ddaghero@polito.it

axis, $B_{c2\parallel c}^\sigma$, is higher than that measured by other groups on similar samples [10,11], possibly because of surface effects. Finally, the temperature dependence of the two gaps is obtained with unprecedented accuracy, by separating the partial σ - and π -band contributions to the total conductance by means of a suitable magnetic field.

2. Experimental set up

All the details about the sample preparation are given in the paper by Karpinski *et al.* in this same issue. The MgB_2 single crystals we used for our measurements were about $0.6 \times 0.6 \times 0.04 \text{ mm}^3$ in size, even though the growth technique allows obtaining even larger samples. The crystals were etched with 1% HCl in dry ethanol, to remove possible deteriorated surface layers. The critical temperature of the crystals, measured by AC susceptibility, is $T_c = 38.2 \text{ K}$ with $\Delta T_c \sim 0.2 \text{ K}$.

Possibly because of the extreme hardness of the crystals, point contacts obtained by pressing a metallic tip against the crystal surface were found to fail the essential requirements of reproducibility and mechanical stability upon thermal cycling. Therefore, we made the contacts by using as a counterelectrode either a small drop of silver conductive paint ($\phi \lesssim 50 \mu\text{m}$) or a small spot of indium. The control of the junction characteristics (which, in the conventional technique, is obtained by moving the tip) was a little more difficult in this case. However, by applying short voltage pulses we were able to change the characteristics of the contact, until satisfactory stability and reproducibility were attained.

Of course, the apparent size of our contacts is much greater than that required to have ballistic transport across the junction [12]. Actually, the effective electrical contact occurs via parallel micro-bridges in the spot area, that can be thought of as Sharvin contacts. This assumption is supported *a posteriori* by the absence of heating effects in the conductance curves of all our junctions. Moreover, by using in the Sharvin formula the experimental resistance of our contacts (that always fell in the range $10 \div 50 \Omega$) the estimated mean free path $\ell = 600 \text{ \AA}$, and the residual resistivity $\rho_0 \approx 2 \mu\Omega \text{ cm}$ [11] one obtains that, at

least in the higher-resistance junctions, the transport is ballistic even if a single contact is established.

The contacts were positioned on the crystal surfaces so as to inject the current along the c axis or along the ab planes. In the following, we will refer to them as “ c -axis contacts” and “ ab -plane contacts”. Notice that, when the potential barrier at the interface is small as in our case, the current is injected in a cone whose angle is not negligible, and becomes equal to $\pi/2$ in the ideal case of no barrier. Anyway, the probability for electrons to be injected along an angle ϕ in the cone is proportional to $\cos \phi$ [13] so that the (main) direction of current injection can still be defined.

3. Experimental results and discussion

3.1. Magnetic field parallel to the c axis

Figure 1 shows the normalized conductance curves of an ab -plane contact, for increasing intensities of the magnetic field applied parallel to the c axis. The differential conductance dI/dV was numerically calculated from the measured $I - V$ characteristic of the junction. The normalization was made by dividing the experimental dI/dV vs. V curves by the linear or quartic function that best fits them for $|V| > 30 \text{ meV}$. The zero-field curve shows two peaks at $V \simeq \pm 2.7 \text{ mV}$ and $V \simeq \pm 7.2 \text{ mV}$, clearly related to the two gaps Δ_π and Δ_σ , respectively. On increasing the magnetic field intensity, the peaks related to the smaller gap, Δ_π , are quickly suppressed, and they finally disappear at $B = \mu_0 H \simeq 1 \text{ T}$. On the contrary, the features connected to the large gap, Δ_σ , look practically unchanged. The whole shape of the conductance curves changes very little if the field slightly exceeds the value $B = 1 \text{ T}$, suggesting that in this magnetic-field region the σ band is quite robust. On further increasing the field intensity, the two peaks corresponding to Δ_σ decrease in amplitude and gradually shift to lower energies, i.e. the large gap gradually closes. At $B = 4 \text{ T}$, however, the normalized conductance is still far from being flat. This means that, at the liquid helium temperature, the upper critical field of the σ band for $\mathbf{B} \parallel c$ is greater than 4 Tesla, in

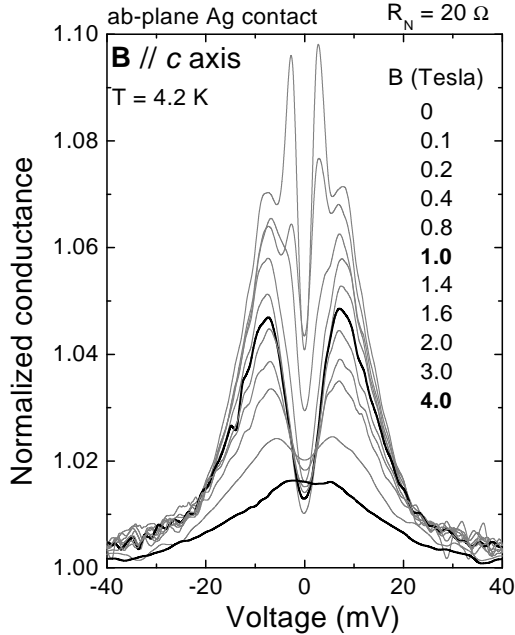


Figure 1. Effect of a magnetic field of increasing intensity, applied parallel to the c axis, on the conductance curves of a Ag/MgB₂ point contact with current injection mainly along the ab plane. All the curves were measured at $T = 4.2$ K. Thick black lines represent the experimental curves at $B = 1$ T and $B = 4$ T.

contrast to the value $H_{c2}^{\parallel c} = 30$ kOe given by recent torque magnetometry [10] and thermal conductivity measurements [11]. The possible reason for this discrepancy will be discussed later on.

Let us discuss for a while the quick suppression of the small-gap features and their disappearance at $B=1$ T. This result was already obtained by point-contact measurements in polycrystalline samples [14], and was interpreted as due to the selective suppression of the superconductivity in the π bands. In our case, the use of single crystals allows giving more convincing arguments to support this interpretation, i.e. to show that the magnetic field of 1 Tesla really destroys the superconductivity in the π bands, without affecting the σ bands.

As a matter of fact, in Figure 2 the zero-field

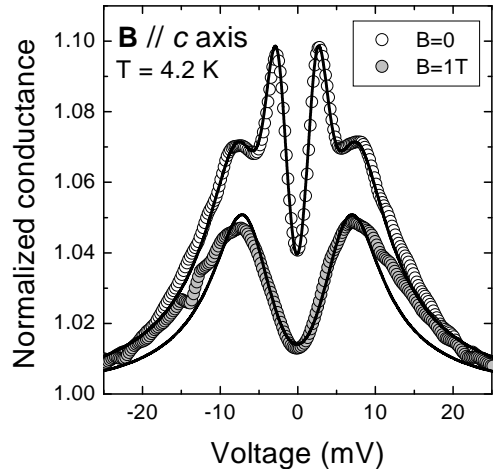


Figure 2. The experimental normalized conductance curves at $B = 0$ (open symbols) and $B = 1$ T (filled symbols) already reported in Fig. 1 compared to the theoretical curves. The solid line superimposed to the upper curve is a best-fitting BTK function (see eq.1). The solid line superimposed to the lower curve is *not* a best-fitting curve, but the function obtained from the previous one by taking $\sigma_\pi = 1$ (see eq.2). For details see the text.

curve (open symbols) and the curve in a field of 1 T (filled symbols) are compared. The solid line superimposed to the former is its best-fitting curve obtained with the BTK model [15] generalised to the case of two bands, in which the *normalized* conductance σ is expressed by a weighed sum of the partial BTK conductances of the π and σ bands:

$$\sigma = w_\pi \sigma_\pi + (1 - w_\pi) \sigma_\sigma. \quad (1)$$

In practice, the total conductance across the junction is thought of as the parallel of two (independent) channels. Here w_π is the weight of the channel connected to the π band, i.e. the partial contribution of the π band to the total conductance. w_π is a function of the plasma frequencies ω_p^σ and ω_p^π , that are much different in the ab -plane and along the c axis. As a result, w_π depends on the angle φ between the direction of current injection and the boron planes [3]. For current injection purely along the ab plane, the value $w_\pi = 0.66$ is

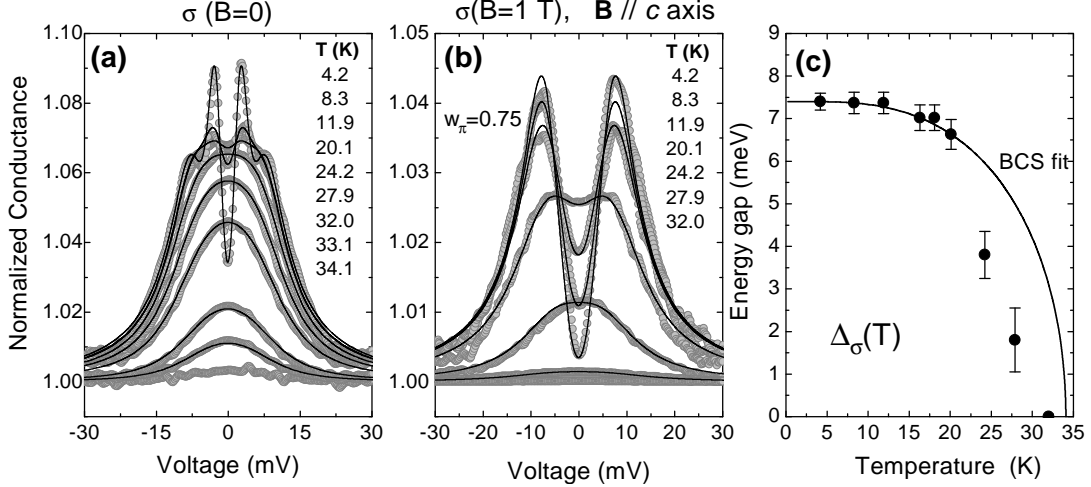


Figure 3. (a) Temperature dependence of the experimental normalized conductance of a ab -plane Ag contact ($R_N = 20 \Omega$). Solid lines are the best-fitting functions given by eq.1. (b) Same as in (a) but with a magnetic field of 1 Tesla applied parallel to the c axis. Solid lines represent the best-fitting curves given by eq.2. (c) Thermal evolution of the large gap Δ_σ as obtained from the fit of the curves in (b).

theoretically predicted [3].

The fitting function expressed by eq. 1 contains 7 adjustable parameters (Δ_σ and Δ_π , the broadening parameters Γ_σ and Γ_π , the barrier transparency coefficients Z_σ and Z_π , plus the weight factor w_π) so there is some uncertainty in the choice of the best-fitting values, especially as far as $Z_{\sigma,\pi}$ and $\Gamma_{\sigma,\pi}$ are concerned. The curve superimposed to the zero-field conductance in Fig. 2 was obtained by using: $\Delta_\pi = 2.8$ meV, $\Delta_\sigma = 7.2$ meV, $Z_\pi = 0.48$, $Z_\sigma = 0.94$, $\Gamma_\pi = 1.49$ meV, $\Gamma_\sigma = 3.3$ meV, and finally $w_\pi = 0.75$. The gap amplitudes agree very well with those predicted by the two-band model [3]. The disagreement between the predicted value of w_π (0.66) and that given by the fit (0.75) is simply due to the fact that, as previously pointed out, the current is injected within a solid angle rather than along a precise direction. As a matter of fact, it can be shown that the value $w_\pi = 0.75$ is compatible with an injection cone about 26° wide [16].

If the superconductivity in the π band is destroyed without affecting the σ band, the total conductance across the junction is expressed by:

$$\sigma = w_\pi + (1 - w_\pi)\sigma_\sigma. \quad (2)$$

which is obtained by taking $\sigma_\pi=1$ in eq.1, and

thus only contains the free parameters Δ_σ , Γ_σ and Z_σ , plus the weight factor w_π . This is indeed the functional form of the curve shown in Fig.2, superimposed to the conductance curve at $B = 1$ Tesla. All the parameters are unchanged with respect to the zero-field curve, apart from the barrier parameter that was set to $Z_\sigma = 0.56$ to adjust the height of the theoretical curve. It is clear that this function reproduces both the position of the conductance peaks and the shape of the conductance well around zero bias. This demonstrates that a field of 1 Tesla parallel to the c axis really destroys the superconductivity in the π band, without affecting the amplitude of the σ -band gap.

One can now wonder whether this is true also when the temperature is increased, or rather a temperature $T^* < T_c$ exists at which also the σ bands start being affected by the field. Fig. 3 reports the temperature dependence of the experimental curves of the same ab -plane contact discussed so far, in zero field (a) and in the presence of a field of 1 Tesla parallel to the c axis (b). Even at a first sight, it is clear that the curves in zero field become almost flat at $T = 34.1$ K, – which is therefore close to the critical temperature of the junction – while the curves in the presence

of the field – that only contain the σ -band conductance – flatten at $T = 32$ K. This suggests by itself that the magnetic field causes the transition to the normal state at a temperature lower than T_c . This conclusion can be further supported by extracting the temperature dependence of Δ_σ from the conductance curves in Fig. 3b, which requires fitting the experimental curves. The solid lines superimposed to the experimental data in (a) and (b) represent the relevant best-fitting curves obtained by using eq.1 and eq.2, respectively. In both cases, the weight w_π was taken as temperature-independent. The barrier parameters Z_σ and Z_π were kept (almost) constant at the increase of the temperature. Instead, the broadening parameters Γ_π and Γ_σ given by the fit increase with T . In the case of Fig. 3a, Γ_π varies between 1.49 and 2.29 meV, and Γ_σ increases from 3.3 up to 3.6 meV; Z_σ and Z_π vary from 0.94 to 0.8 and from 0.48 to 0.33, respectively. In the case of Fig. 3b, instead, Γ_σ is equal to 3.7 meV at low T and increases rapidly on heating, while Z_σ remain in the range between 0.6 and 0.45.

The thermal evolution of Δ_σ , obtained by fitting the curves in Fig. 3b with the three-parameter function given by eq. 2, is reported in Fig. 3c (circles) together with a BCS-like curve (solid line). It is clear that the points sudden deviate from the BCS behaviour at $T^* \sim 20$ K. Based on previous determinations of the temperature dependence of Δ_σ in zero field [16], we can rather safely assume that such a large deviation is due to the progressive closing of the large gap due to the magnetic field. At $T = 32$ K, the σ -band gap disappears: this means that, at this temperature, $B_{c2}^{\parallel c} \sim 1$ T. Again, this value is larger than that recently measured in the same crystals by other groups [10,11].

3.2. Magnetic field parallel to the ab planes

Fig. 4 shows the conductance curves of a ab -plane In contact as a function of the intensity of the magnetic field, applied parallel to the ab planes. Exactly as in Fig.1, the small-gap features are very easily disrupted by the field. At $B=1$ T, Δ_π completely vanishes while Δ_σ remains unchanged. Based on arguments similar

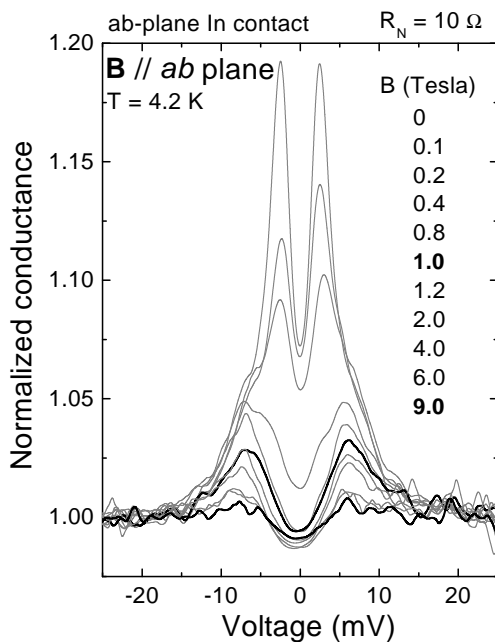


Figure 4. Magnetic-field dependence of the low-temperature normalized conductance curves of a ab -plane In contact. The magnetic field is applied parallel to the ab plane. Thick lines represent the curves at 1 T and 9 T.

to those used in the $\mathbf{B} \parallel c$ case, we can conclude that, at the liquid helium temperature, the upper critical field of the π bands is isotropic, as shown in ref. [17], and takes the value $B_{c2}^\pi = \mu H_{c2}^\pi \simeq 1$ T. Contrary to what happens in a magnetic field applied parallel to the c axis, the conductance peaks associated to the σ -band gap remain well distinguishable up to 9 T. A small decrease in the gap amplitude is observed above 4 T, together with an increase in the zero-bias conductance. It looks thus clear that, at 4.2 K, the critical field of the σ band in the $\mathbf{B} \parallel ab$ case is much greater than 9 T, in agreement with other experimental findings.

As already done in the $\mathbf{B} \parallel c$ case, let us check whether the robustness of the σ bands upon application of a field of 1 Tesla persists at the increase of the temperature. Figure 5 reports the temperature evolution of the normalized conductance curves (symbols) in zero field (a), and in the presence of a field of 1 Tesla (b) parallel to

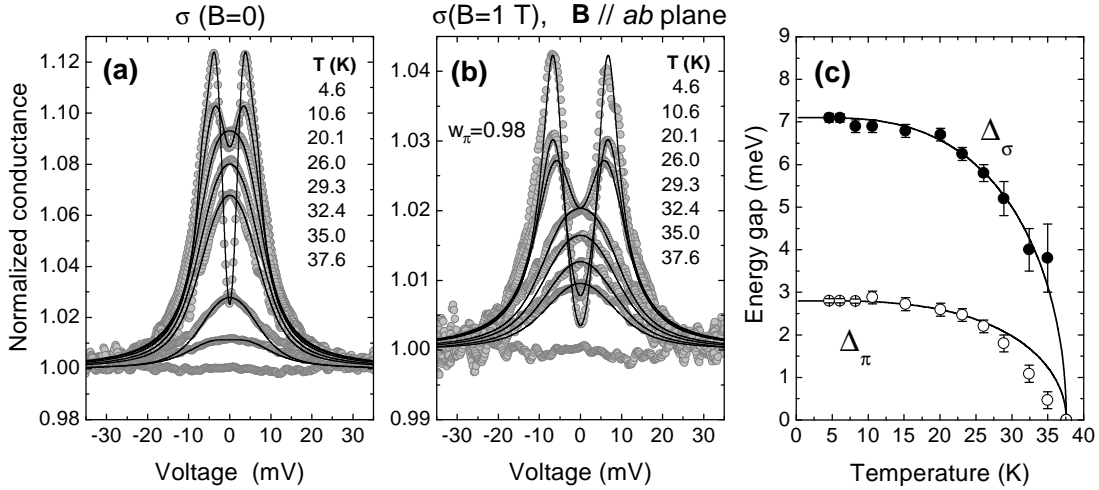


Figure 5. (a) Temperature dependence of the experimental normalized conductance of a c -axis In contact ($R_N = 50 \Omega$). Solid lines are the best-fitting curves of the form given in eq.1. (b) Same as in (a) but in a magnetic field of 1 Tesla applied parallel to the ab plane. Lines: best-fitting curves expressed by eq.2. (c) Temperature dependence of the large gap Δ_σ from the fit of the curves in (b), and of the small gap Δ_π from the fit of the difference between the curves in (a) and (b) (see ref.[16] for details).

the ab plane. It is clearly seen that, in this case, all the curves become flat at the same temperature $T = 37.6$ K – which is the critical temperature of the junction – indicating that the superconductivity in the σ band survives up to T_c even in the presence of the field. Solid lines in Figs. 5a and 5b represent the best-fitting curves obtained by using eqs.1 and 2, respectively. The value of the weight $w_\pi = 0.98$ was determined by fitting the zero-field, low-temperature curve and then kept constant². Let us disregard the values of the fitting parameters of the zero-field curves, as they are not essential for our reasoning. As far as the curves in Fig. 5b are concerned, the low-temperature values of the fitting parameters are: $\Delta_\pi = 7.1$ meV, $\Gamma_\sigma = 1.75$ meV and $Z_\sigma = 0.58$. At the increase of the temperature, Γ_σ regularly increases up to 4.2 meV close to T_c , while Z slightly decreases down to 0.35. The temperature dependence of Δ_σ obtained by the fit is reported in Fig. 5c (solid symbols) and compared to a BCS-like curve (solid line). In agreement

with previous experimental findings and theoretical predictions [2,3], the large gap is found to follow rather well the BCS curve. Incidentally, this confirms *a posteriori* that the σ -band gap is not affected by the field of 1 Tesla even at temperatures rather close to T_c . Also notice the much smaller error on the gap values with respect to measurements in polycrystalline samples, due to the reduction in the number of adjustable parameters (from 6 to 3) obtained by removing the π band gap by means of the field [16].

An highly accurate determination of the temperature evolution of Δ_π is possible as well, by subtracting from the total conductance the partial contribution of the σ band. In practice, each experimental curve in Fig. 5b is subtracted from the curve in zero field measured at the same temperature, as discussed elsewhere [16], and the resulting curve is fitted by a function of the form $\sigma = w_\pi(\sigma_\pi - 1)$, with $w_\pi = 0.98$. The temperature dependence of Δ_π obtained from the fit is shown in Fig. 5c (open symbols) and compared to a BCS-like behaviour (solid line). At $T \gtrsim 20$ K, Δ_π deviates from the BCS curve of an amount which is well greater than our experimental un-

²For current injection purely along the ab planes the predicted value of the weight is $w_\pi = 0.99$. Our value is compatible with a current injection cone of about 60°.

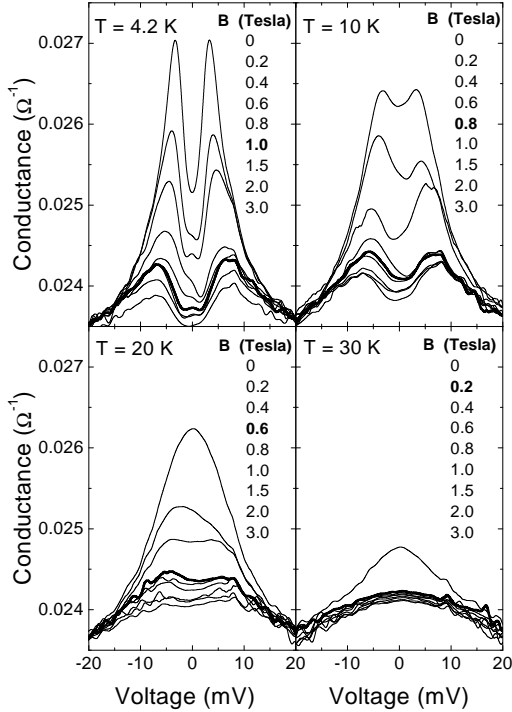


Figure 6. Unnormalized conductance curves of a c -axis In contact ($R_N \sim 42 \Omega$) in a magnetic field of increasing intensity, applied parallel to the ab plane. Each panel refers to a different temperature, indicated in the graph.

certainty. This deviation is indeed predicted by the two-band model [2,3] but its unquestionable determination was impossible so far, because of the very large error affecting the gap values near T_c .

3.3. Temperature dependence of B_{c2}^π

Finally, let us determine the temperature evolution of the critical field of the π band, whose value at 4.2 K has been evaluated by analyzing the curves in Figs. 1 and 4. Fig. 6 reports the unnormalized (i.e., as-measured) conductance curves of a c -axis contact, in the presence of a magnetic field applied parallel to the ab planes, at four temperatures: 4.2, 10, 20 and 30 K. Based on our previous finding that $B_{c2\parallel ab}^\pi = B_{c2\parallel c}^\pi = 1$

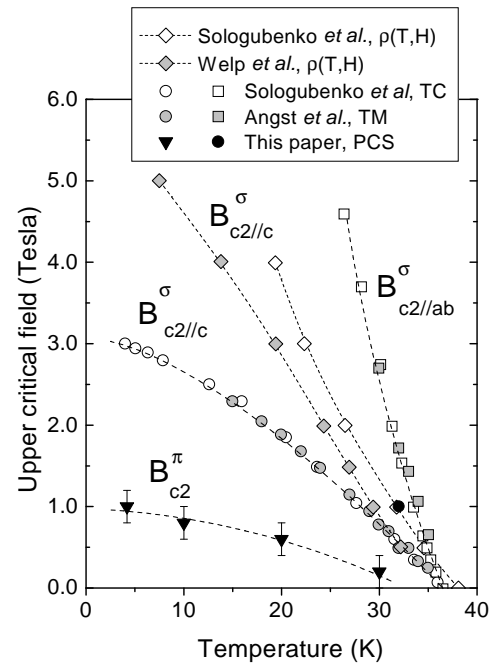


Figure 7. Phase diagram of MgB_2 as it results from different kinds of measurements (TM = torque magnetometry, TC = thermal conductivity, PCS = point-contact spectroscopy, $\rho(T, H)$ = resistivity) carried out in single crystals. Lines are only guides to the eye.

T at 4.2 K, and on the essentially isotropic character of the π bands [5,6,7,8,17] we will assume that the above equality holds at any temperature. The use of a c -axis contact emphasizes the π -band contribution to the conductance, but makes it more difficult to distinguish the (very small) σ -band features that survive after the removal of Δ_π . However, we expect that, just above B_{c2}^π , the conductance curves should be (relatively) field-independent, as long as the residual σ -band gap is not suppressed. The curve that marks the beginning of this “saturation” is represented by a thick curve in the four panels of Fig. 6³. At 4.2, 10 and 20 K a residual gap-like feature is clearly observed in these curves, thus indicating the persistence of superconductivity in the σ bands. At

³Notice that only the curves at some representative field intensities are reported for clarity.

$T = 30$ K the saturation occurs at $B \simeq 0.2$ T and above this field only minor changes in the conductance are observed. Since the upper critical field of MgB_2 in the $\mathbf{B} \parallel ab$ case is, even at this temperature, at least one order of magnitude greater than 0.2 T [10,11,18], there is no doubt that this saturation is due to the removal of the π -band gap alone.

The values of the magnetic field intensities that give rise to this saturation, and that we interpret as B_{c2}^π , are reported in Fig.7 (black triangles) together with the results of torque magnetometry [10], resistivity [11,18] and thermal conductivity measurements [11]. There are two points that are worth mentioning: the clear overestimation of $B_{c2\parallel c}^\sigma$ by transport measurements, and the fact that all the critical fields determined by bulk measurements (e.g. thermal conductivity and torque magnetometry) vanish at a temperature $T < T_c$, where T_c is determined by the resistive transition. These puzzling results have been recently interpreted as due to the existence of an additional phase with enhanced critical parameters (T_c and H_{c2}), probably related to surface effects that seem to be strongly suppressed by in-plane magnetic fields [18]. If this is the case, the results of surface-sensitive measurements might be sensibly different from those of bulk-sensitive techniques. This is an important point in discussing our results, since PCS is intrinsically a surface-sensitive probe. As a matter of fact, the value we determined for $B_{c2\parallel c}^\sigma$ (black circle) is well compatible with the results of resistive measurements by Sologubenko *et al.*, that were carried out on similar single crystals. Moreover, the observation of σ -band superconductivity at 4.2 K in a field of 4 T parallel to the c axis (see fig.1) further supports this picture.

In conclusion, we have presented the results of a systematic study of MgB_2 by means of point-contact spectroscopy in the presence of a magnetic field. The use of single crystals has allowed us to control the direction of both the current injection and the applied magnetic field. Consequently, we have been able to study the effect of the magnetic field on each band separately, and to determine for the first time the temperature dependence of the upper critical field of the isotropic

π bands. As far as the σ bands are concerned, the effect of the magnetic field has been confirmed to be strongly anisotropic. The obtained value of the upper critical field $B_{c2\parallel c}^\sigma$ is higher than that measured on the same crystals by torque magnetometry and thermal conductivity, but agrees very well with the results of transport measurements. Finally, by exploiting the directionality of the point contacts and the different effect of the magnetic field on the two band systems, we have selectively destroyed the superconductivity in the π bands. This procedure allows separating the partial contributions of the σ and π bands to the total conductance of the point contacts. Fitting each partial conductance with the standard BTK model, we have determined with great accuracy the temperature dependence of the two gaps, confirming the predictions of the two-gap models appeared in literature.

This work was supported by the INFM Project PRA-UMBRA and by the INTAS project "Charge transport in metal-diboride thin films and heterostructures".

REFERENCES

1. H. Suhl, B.T. Matthias, and L.R. Walker, Phys. Rev. Lett. **3**, 552 (1959).
2. A.Y. Liu, I.I. Mazin, and J. Kortus, Phys. Rev. Lett. **87**, 87005 (2001).
3. A. Brinkman *et al.*, Phys. Rev. B **65**, 180517(R) (2001).
4. I.I. Mazin *et al.*, cond-mat/0204013.
5. J. Kortus *et al.*, Phys. Rev. Lett. **86**, 4656 (2001).
6. S.V. Shulga *et al.*, cond-mat/0103154.
7. J.M. An and W.E. Pickett, Phys. Rev. Lett. **86**, 4366 (2001).
8. Y. Kong, O.V. Dolgov, O. Jepsen, and O.K. Andersen, Phys. Rev. B **64**, 020501(R) (2001).
9. C. Buzea and T. Yamashita, Supercond. Sci. Technol. **14**, R115 (2001).
10. M. Angst *et al.*, Phys. Rev. Lett. **88**, 167004 (2002).
11. A.V. Sologubenko *et al.*, Phys. Rev. B **66**, 014504 (2002).
12. A.M. Duif, A.G.M. Jansen, and P. Wyder, J. Phys.: Condens. Matter **1**, 3157 (1989).
13. S. Kashiwaya and Y. Tanaka, Rep. Prog. Phys. **63**, 1641 (2000).
14. P. Szabó *et al.*, Phys. Rev. Lett. **87**, 137005 (2001).
15. G.E. Blonder, M. Tinkham, and T.M. Klapwijk, Phys. Rev. B **25**, 4515 (1982).
16. R.S. Gonnelli *et al.*, cond-mat/0208060.
17. F. Bouquet *et al.*, cond-mat/0207141.
18. U. Welp *et al.*, cond-mat/0203337.